Journal of Power Sources 193 (2009) 155–159

Contents lists available at ScienceDirect

Journal of Power Sources

journal homepage: www.elsevier.com/locate/jpowsour

Short communication

Phase stability and conductivity of $Ba_{1-y}Sr_yCe_{1-x}Y_xO_{3-\delta}$ solid oxide fuel cell electrolyte

I-Ming Hung*, Hao-Wei Peng, Shao-Lou Zheng, Chun-Peng Lin, Jun-Sheng Wu

Yuan Ze Fuel Cell Center/Department of Chemical Engineering and Materials Science, Yuan Ze University, No. 135, Yuan-Tung Road, Chungli, Taoyuan 320, Taiwan

ARTICLE INFO

Article history:
Received 14 October 2008
Received in revised form 11 February 2009
Accepted 16 February 2009
Available online 4 March 2009

Keywords:
Solid oxide fuel cell
Phase stability
Conductivity
Perovskite
$Ba_{1-y}Sr_yCe_{0.8}Y_{0.2}O_{3-\delta}$

ABSTRACT

The structure, phase stability, and electrical properties of $BaCe_{1-x}Y_xO_{3-\delta}$ ($x = 0$–0.4) in humidity air and CO_2 atmosphere are investigated. XRD results indicate that the $BaCe_{0.9}Y_{0.1}O_{3-\delta}$ sample has a symmetric cubic structure, and its phase changes to tetragonal as the Y^{3+} doping amount increases to 20 mol%. The conductivity of $BaCe_{1-x}Y_xO_{3-\delta}$ increases with temperature, and it depends on the amount of yttrium doping and the atmosphere. $BaCe_{0.8}Y_{0.2}O_{3-\delta}$ exhibits the highest conductivity of 0.026 S cm^{-1} at 750 °C. The activation energy for conductivity depends on yttrium doping amount and temperature. The conductivity of $BaCe_{0.8}Y_{0.2}O_{3-\delta}$ is 0.025 S cm^{-1} in CO_2 atmosphere at 750 °C which is 3.8% lower than that in air due to reactions with CO_2 and $BaCO_3$ and the CeO_2 impure phases formed. The structure of $BaCe_{0.8}Y_{0.2}O_{3-\delta}$ is unstable in water and decomposes to $Ba(OH)_2$ and CeO_2 phases. It is found that the activation energy of samples in CO_2 atmosphere is higher than that of sample in air. Sr-doped $Ba_{1-y}Sr_yCe_{0.8}Y_{0.2}O_{3-\delta}$ ($y = 0$–0.2) is prepared to improve the phase stability of $BaCe_{0.8}Y_{0.2}O_{3-\delta}$ in water. The conductivity of $Ba_{0.9}Sr_{0.1}Ce_{0.8}Y_{0.2}O_{3-\delta}$ is 0.023 S cm^{-1} at 750 °C which was 11% lower than that of $BaCe_{0.8}Y_{0.2}O_{3-\delta}$, however, the phase stability of $Ba_{0.9}Sr_{0.1}Ce_{0.8}Y_{0.2}O_{3-\delta}$ is much better than that of $BaCe_{0.8}Y_{0.2}O_{3-\delta}$ in water.

1. Introduction

A solid oxide fuel cell (SOFC) is regarded as a highly efficient and clean power-generation system because of its high conversion efficiency and low pollution [1]. A conventional high-temperature SOFC (HT-SOFC) is based on the 8-mol% yttria-stabilized zirconia (YSZ) electrolyte, which requires operation at a high-temperature range of 800–1000 °C. However, such a high operation temperature causes many problems such as high cost, limitation of the materials for sealing and the current connector, reactions between the components, thermal expansion mismatch, and a long start-up and shut-off period, etc. Therefore, there has been considerable interest in SOFCs operating at an intermediate temperature range of 600–800 °C. A key issue in the development of intermediate temperature SOFCs (IT-SOFCs) is the use of a highly ion conductive electrolyte at intermediate temperatures. Recently, high-temperature protonic conductors (HTPCs) have gained considerable attention because they are used as solid electrolytes for electrochemical devices such as IT-SOFCs, hydrogen sensors, hydrogen pumps, steam electrolyzers, etc.

There are many kinds of perovskite-type oxides that have oxygen vacancies and p-type conductivity. Perovskite-type oxides such as $BaZrO_3$, $SrZrO_3$, $SrCeO_3$ and $BaCeO_3$ doped with a rare-earth oxide are known to be proton conductors. It was found that protonic conductivity appears as electronic conductivity decreases for these ceramics in water vapor or a hydrogen atmosphere. Cation-doped $BaCeO_3$ attracted great interest in the 1980s and 1990s due to their high proton conductivity at 400–700 °C. Iwahara et al. demonstrated that $BaCeO_3$ has the highest protonic conductivity among these HTPCs [2–4]. $BaCeO_3$-based HTPCs have been considered good candidate materials for IT-SOFC electrolytes because of their high ionic conductivity. The power density of IT-SOFCs based on the $BaCeO_3$ electrolyte varied from 50 to 1400 mW cm^{-2} [5–9]. However, cation-doped $BaCeO_3$ has not yet been commercialized, compared with the traditional oxide-ion conductors such as yttria-stabilized zirconia and doped ceria, it has a chemical stability problem under SOFC operation conditions, such as in wet air and an atmosphere containing CO_2. The stability of $BaCeO_3$ has been examined by Virkar and co-workers [10,11] and it was concluded that the $BaCeO_3$ decomposed to form $BaCO_3$, $Ba(OH)_2$ and CeO_2 in a wet CO_2 atmosphere. Recently, a fuel cell based on $BaCe_{0.8}Y_{0.2}O_3$ electrolyte was demonstrated. The power density was 0.9 and 1.4 W cm^{-2} at the operating temperatures of 400 and 600 °C, respectively [12–15].

Many reports with respect to $BaCeO_3$-based oxides have been published, but there were large differences among them in their discussion of its properties. It is believed that its properties are strongly influenced by the type and ratio of the dopants and the method of synthesis.

In order to exhibit proton conduction for $BaCeO_3$, doping with lower valency cations, as well as introducing water vapor, is essen-

* Corresponding author. Tel.: +886 3 4638800x2569; fax: +886 3 4630634.
E-mail address: imhung@saturn.yzu.edu.tw (I.-M. Hung).

0378-7753/$ – see front matter © 2009 Elsevier B.V. All rights reserved.
doi:10.1016/j.jpowsour.2009.02.061

tial. A trivalent dopant such as yttria can lead to the creation of oxygen vacancies, as given by:

$$2Ce_{Ce}^{X} + O_o + Y_2O_3 \rightarrow 2Y_{Ce}' + V_o^{\bullet\bullet} + 2CeO_2 \quad (1)$$

These oxygen vacancies interact with the water vapor in the use environment to form protons, as given by:

$$V_o^{\bullet\bullet} + O_o^{X} + H_2O(gas) \leftrightarrow 2OH_o^{\bullet} \quad (2)$$

The water incorporation results in the uptake of two protons per oxygen vacancy in the structure. The concentration of protons in the material depends on the oxygen vacancy concentration and, therefore, also on the dopant content. The protons are quasi-free and generally not bound to any particular oxygen ions; they can migrate from one oxygen ion to another in the nearest neighbor oxygen ion in the lattice. This migration mechanism results in high proton conductivity (as high as $10^{-2}\ \Omega^{-1}\ cm^{-1}$ at 500 °C) for these HTPC oxides [16]. The doped $BaCeO_3$ exhibited both ion and p-type electrical conductivity at higher temperatures in a high PO_2 and dry atmosphere, whereas it was a pure ion conductor at lower temperatures in a low PO_2 and moist atmosphere. The conductivity mechanism in doped perovskites was discussed was detail by Ma et al. [17] and Haile et al. [13]. These results show that protons are actually associated with oxide ions to form hydroxide ions.

It is essential to ensure that the materials have thermodynamic or at least long-term kinetic stability in addition to good conductivity in the application environment for the electrolyte of SOFC. As many researchers have pointed out, a concern for $BaCeO_3$ is chemical stability. Stability problems in atmospheres containing water and CO_2 are generally suspected because of the thermodynamic instability of $BaCeO_3$ towards these gases. For pure $BaCeO_3$, the standard Gibbs free energy change of the reaction of $BaCeO_3$ with water is zero at 403 °C and is negative at lower temperatures. $BaCeO_3$ also tends to react with carbon dioxide to form barium carbonate and cerium oxide; the standard Gibbs free energy is zero at 1041 °C and negative at lower temperature [18]. Therefore, $BaCeO_3$ is thermodynamically unstable in high partial pressure of water and carbon dioxide at low temperatures. Recently, many effects of adjusting the chemical composition or coating a protection layer to prevent the degradation of the $BaCeO_3$-based proton conductor have been determined [7].

A high protonic conductivity with stable structure in different atmospheres is considered to be a key problem for HTPC materials for SOFC applications. The aim of the present study is to clarify the characteristics and conductivity of $BaCe_{1-x}Y_xO_{3-\delta}$ in both air and CO_2 atmospheres at intermediate temperatures (450–750 °C) in order to obtain a better $BaCeO_3$-based oxide solid electrolyte. In addition, strontium-doped $Ba_{1-y}Sr_yCe_{0.8}Y_{0.2}O_{3-\delta}$ (y = 0–0.2) was prepared to improve the phase stability of $BaCe_{0.8}Y_{0.2}O_3$ in water.

2. Experimental

The yttria and strontium-doped barium cerates were prepared by conventional solid-state synthesis techniques. Stoichiometric ratios of high purity oxide powders of $BaCO_3$ (J.T. Baker, 99.9%), CeO_2 (Alfa, 99.9%), SrO (Alfa, 99.99%) and Y_2O_3 (Alfa, 99.99%) were mixed and ball milled in ethanol for 24 h. The dried powders were subsequently calcined at 1300 °C in air for 12 h. The calcined powders were pressed under 20 kg cm^{-2} into approximately 1 cm diameter and 2 mm thick pellets. The samples were subsequently isostatically pressed at 25 MPa and finally sintered at 1600 °C for 4 h in air to obtain specimens with relative densities higher than 95%.

The phase identification of the BSCF powders was performed with a powder diffractometer (LabX, XRD-6000) with Ni-filtered Cu K_α radiation and the diffraction angle from 20° to 80° with a step of 0.01° and a rate of 1° min^{-1}, and on the beam line 01C2 at the National Synchrotron Radiation Research Center (NSRRC) in Taiwan, operating at an energy of 25 keV (λ = 0.4959 Å). The conductivity measurement and electrochemical impedance spectra (EIS) were made under wet air and 100% carbon dioxide in a temperature range of 450–750 °C by a dc two-probe method and the complex impedance was determined using an impedance analyzer (HIOKI, 3532-50) with condition of 100 mV, 1000 kHz to 0.01 Hz frequency.

3. Results and discussion

The XRD patterns of $BaCe_{1-x}Y_xO_{3-\delta}$ calcined at 1300 °C for 12 h are shown in Fig. 1. Fig. 1(a) gives the XRD pattern of $BaCe_{0.9}Y_{0.1}O_{3-\delta}$, where the structure belongs to a perovskite cubic structure. The peaks include the (1 1 0), (1 1 1), (2 0 0), (2 1 1), (2 2 0), (3 1 0), (2 2 2), and (3 2 1) reflections. The lattice parameter a is about 4.391 Å, which is little larger than that for $BaCeO_3$ (4.377 Å, JCPDS no. 75-0431). For the yttria-doped $BaCeO_3$ powders, it was expected that the lattice parameter would be a function of the yttrium doping concentration. The ion radius of Y^{3+} is 0.92 Å, which is greater than that of Ce^{4+} (0.9 Å); therefore, the lattice parameter and the unit cell volume should increase with the doping Y^{3+} concentration. However, oxygen vacancies were created in the lattice because, Y^{3+} doping in $BaCeO_3$, the unit cell can also shrink. Therefore, the unit cell of $BaCe_{1-x}Y_xO_{3-\delta}$ can either increase or decrease with an increasing Y^{3+} doping concentration, depending upon the contributions of these two opposing factors. As the Y^{3+} doping amount increased above 20 mol%, it was observed that certain XRD peaks split, confirming that samples had a single-phase tetragonal perovskite-type structure. Iwahara et al. [19] studied the mixed conduction of Yb, Y, Dy, Gd, Sm, and Nd-doped $BaCeO_3$, and reported that the proton transference number decreased while the oxygen ion transference number increased with a larger doping ionic radius. The reason for this is the enlarged spacing volume due to doping with large ionic radius elements.

The conductivity of $BaCe_{1-x}Y_xO_{3-\delta}$ samples as a function of temperature in air is shown in Fig. 2. The conductivity of all samples increased with an increase in the measured temperature, indicated that the $BaCe_{1-x}Y_xO_{3-\delta}$ is an ionic conductor. It was

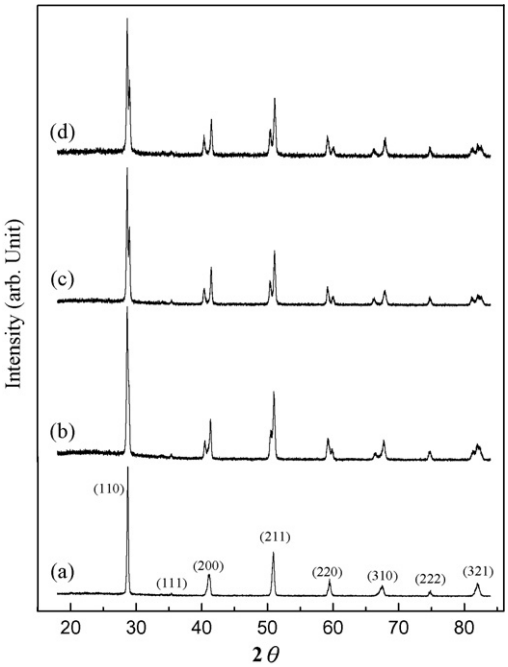

Fig. 1. XRD patterns of (a) $BaCe_{0.9}Y_{0.1}O_{3-\delta}$, (b) $BaCe_{0.8}Y_{0.2}O_{3-\delta}$, (c) $BaCe_{0.7}Y_{0.3}O_{3-\delta}$, and (d) $BaCe_{0.6}Y_{0.4}O_{3-\delta}$ samples calcined at 1300 °C for 12 h.

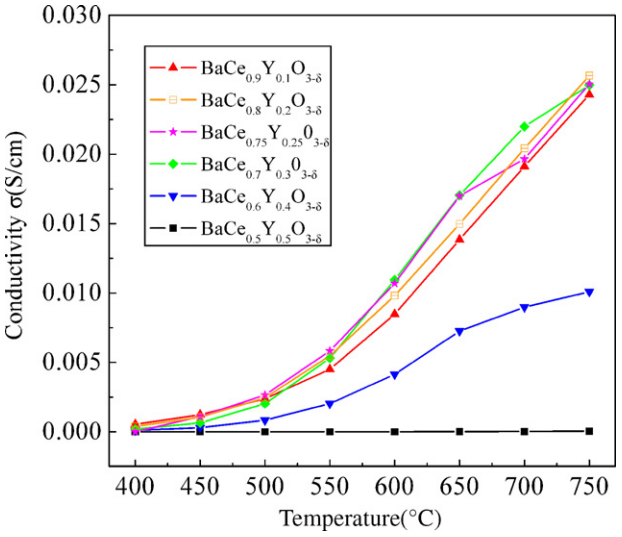

Fig. 2. Conductivity of $BaCe_{1-y}Y_yO_{3-\delta}$ at different temperatures in air.

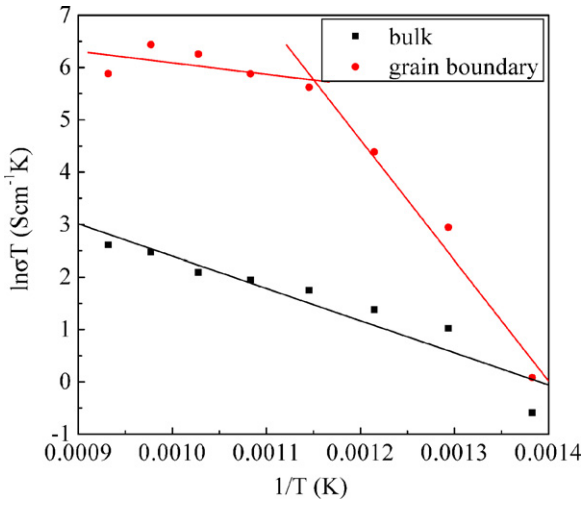

Fig. 4. Arrhenius plot of bulk and grain boundary conductivity of $BaCe_{0.8}Y_{0.2}O_{3-\delta}$ in air.

found that the conductivities of $BaCe_{0.9}Y_{0.1}O_{3-\delta}$, $BaCe_{0.8}Y_{0.2}O_{3-\delta}$, and $BaCe_{0.7}Y_{0.3}O_{3-\delta}$ are much higher than that of $BaCe_{0.6}Y_{0.4}O_{3-\delta}$. The resulting conductivity of the $BaCe_{0.7}Y_{0.3}O_{3-\delta}$ at 550–700 °C is higher than that of $BaCe_{0.9}Y_{0.1}O_{3-\delta}$ and $BaCe_{0.8}Y_{0.2}O_{3-\delta}$. The $BaCe_{0.8}Y_{0.2}O_{3-\delta}$ exhibited the maximum conductivity of 0.026 S cm^{-1} at 750 °C which is much higher than that of the $Ce_{0.8}Sm_{0.2}O_{1.9}$ (SDC) and 16 mol% yttria-doped zirconia (8YSZ). In addition, we compared the maximum conductivity of 0.026 S cm^{-1} of $BaCe_{0.8}Y_{0.2}O_{3-\delta}$ with the $BaCe_{0.75}Y_{0.25}O_{3-\delta}$ reported by Hibino and co-workers [20]. It was found that this data is similar to the data (0.029 S cm^{-1}) reported by Hibino. It is well known that when $BaCeO_3$ is doped with yttrium, it is expected that Y^{3+} ions will replace the Ce^{4+}, creating doubly charged oxygen vacancies. In HTPC, the proton conductivity resulted from oxygen ion vacancies and the dissociative absorption of water. Therefore, the concentration of protonic defects ($OH^{\bullet}_{O}$) in these materials depends on the oxygen ion vacancy concentration, humidity and atmosphere.

The activation energy of the conductivity of $BaCe_{1-x}Y_xO_{3-\delta}$, E_a, was determined by plotting $\ln(\sigma T)$ vs. 1000 T^{-1} following the Arrhenius equation of $\sigma T = A\exp(-E_a/RT)$. Fig. 3 is an Arrhenius plot of the conductivity of $BaCe_{1-x}Y_xO_{3-\delta}$ at 400–750 °C. It is worth noting that the conductivity behavior of all samples shows an apparently

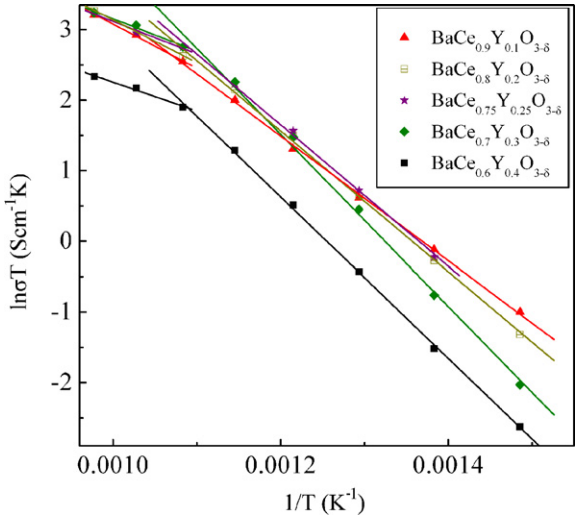

Fig. 3. Arrhenius plot of conductivity of $BaCe_{1-x}Y_xO_{3-\delta}$ in air.

change above 650 °C. An E_a value of 73–101 kJ mol^{-1} is calculated in the low temperature range of 400–650 °C. However, an E_a value of 34–52 kJ mol^{-1} is obtained in the high-temperature range of 650–750 °C. This result indicated that the conductivity mechanism changes as the measured temperature of 650 °C. Dynys reported similar results, but the temperature for the conductivity mechanism change in this study was higher than that reported by Dynys et al. [21]. The probable reasons for conductivity mechanism change are the phase transformations of $BaCe_{1-x}Y_xO_{3-\delta}$ and the charge carrier changes from proton to oxygen-ion in high temperatures. The structure identification and oxygen-ion conductivity at 550–750 °C are still in process.

The conductivity of the bulk and grain boundary of $BaCe_{0.8}Y_{0.2}O_{3-\delta}$ was determined by EIS. The Arrhenius plot of this is shown in Fig. 4. There is only one conductivity mechanism for bulk conductivity in the temperature range of 450–800 °C. The activation energy of bulk conductivity is 51 kJ mol^{-1}. However, there are two conductivity mechanisms for grain conductivity in the temperature ranges of 450–600 and 600–800 °C. The activation energy of grain conductivity is 191 and 18 kJ mol^{-1}, respectively. It was found that the activation energy of grain conductivity is much higher than that of bulk conductivity at low temperatures. This result indicates that the diffusion of protons in the grain boundary is lower than that in bulk at low temperatures; however, the diffusion of oxygen is higher in the grain boundary than that in bulk. Therefore, the conductivity of a nano-sized proton conductor is expected to be improved in large grain boundary area due to low diffusion barrier.

The conductivity of $BaCe_{1-x}Y_xO_{3-\delta}$ samples as a function of temperature in a 100% CO_2 atmosphere is shown in Fig. 5. It was found that the conductivity of $BaCe_{0.8}Y_{0.2}O_{3-\delta}$ is higher than that of other samples and only decreases 3.8% in relation to that of $BaCe_{0.8}Y_{0.2}O_{3-\delta}$ in air. The conductivity of $BaCe_{0.8}Y_{0.1}O_{3-\delta}$, $BaCe_{0.75}Y_{0.25}O_{3-\delta}$ and $BaCe_{0.7}Y_{0.3}O_{3-\delta}$ decreases by 17.6–53.3% compared to their conductivity in air. There is no conductivity behavior for the $BaCe_{0.6}Y_{0.4}O_{3-\delta}$. Fig. 6 gives an Arrhenius plot of the conductivity of $BaCe_{1-x}Y_xO_{3-\delta}$ at 400–750 °C in a 100% CO_2 atmosphere. There are still two conductivity mechanisms from proton conductivity change to oxygen conductivity at about 600 °C; this is similar to the result in air. However, the activation energy of samples in a CO_2 rich atmosphere is little higher than that in air. It is suggested that the chemical reaction between $BaCe_{0.8}Y_{0.2}O_{3-\delta}$ and CO_2 is lower for other samples. Fig. 7 shows the XRD patterns of all samples' heat treatment in 100% CO_2 atmo-

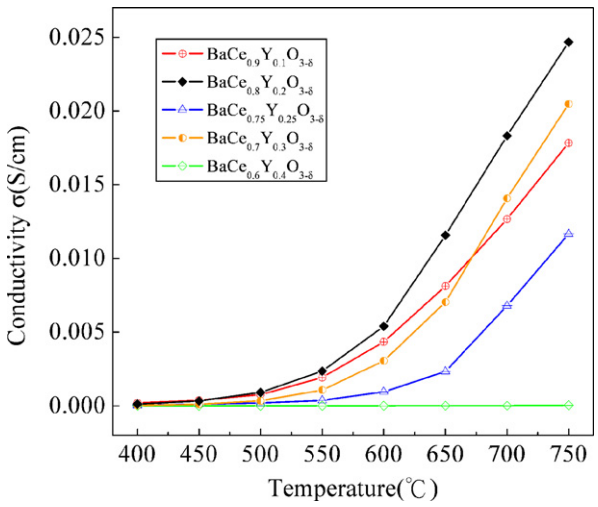

Fig. 5. Conductivity of $BaCe_{1-y}Y_yO_{3-\delta}$ at different temperatures in CO_2 atmosphere.

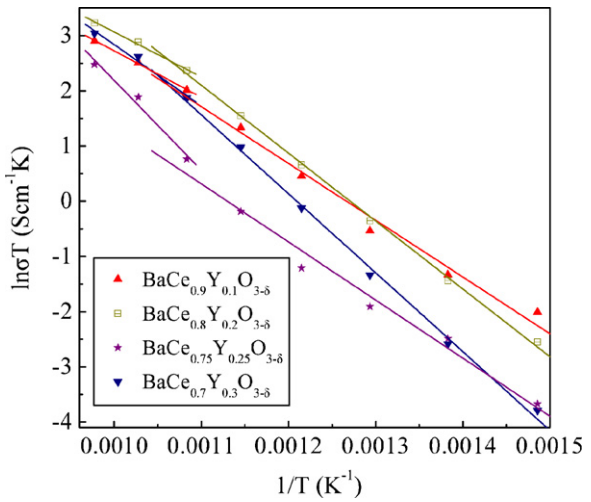

Fig. 6. Arrhenius plot of conductivity of $BaCe_{1-y}Y_yO_{3-\delta}$ in CO_2 atmosphere.

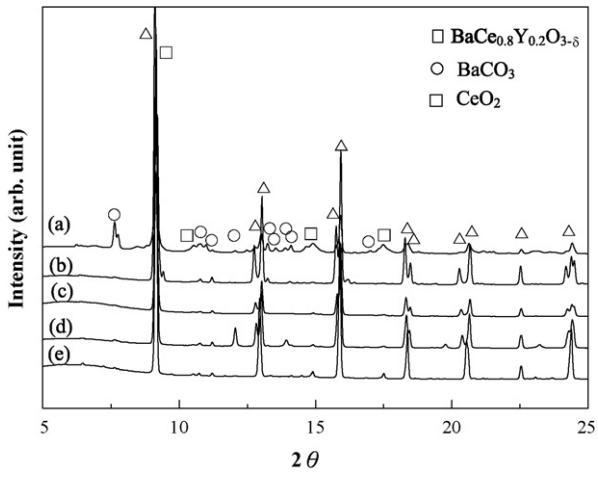

Fig. 7. XRD patterns of (a) $BaCe_{0.6}Y_{0.4}O_{3-\delta}$ (b) $BaCe_{0.7}Y_{0.3}O_{3-\delta}$, (c) $BaCe_{0.75}Y_{0.25}O_{3-\delta}$, (d) $BaCe_{0.8}Y_{0.2}O_{3-\delta}$ and (e) $BaCe_{0.9}Y_{0.1}O_{3-\delta}$ heat treatment in 100% CO_2 atmosphere at 750 °C.

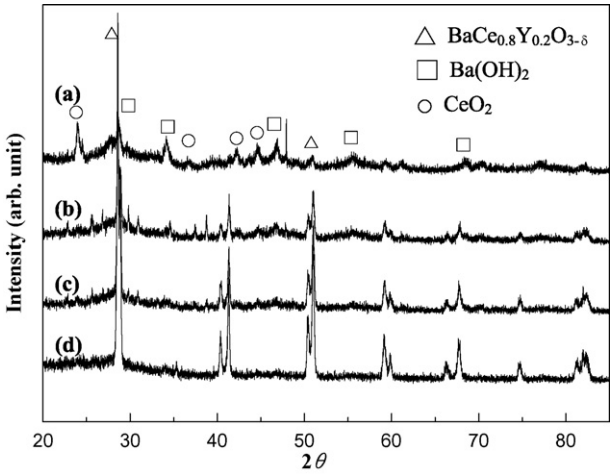

Fig. 8. XRD patterns of $BaCe_{0.8}Y_{0.2}O_{3-\delta}$ exposed to a water vapor-rich environment at 80 °C for (a) 8 h, (b) 6 h, (c) 4 h, and (d) 2 h.

sphere at 750 °C (λ = 0.495942 Å). It was found that only a small amount of $BaCO_3$ impure phases was formed in the $BaCe_{0.9}Y_{0.1}O_{3-\delta}$, $BaCe_{0.8}Y_{0.2}O_{3-\delta}$, $BaCe_{0.75}Y_{0.25}O_{3-\delta}$ and $BaCe_{0.7}Y_{0.3}O_{3-\delta}$ samples. However, a large amount of $BaCO_3$ and CeO_2 impure phases was formed in the $BaCe_{0.6}Y_{0.4}O_{3-\delta}$ sample; this is the main reason that the $BaCe_{0.6}Y_{0.4}O_{3-\delta}$ sample does not exhibit conductivity behavior in a CO_2 atmosphere.

From the result described above, it was found that the $BaCe_{0.8}Y_{0.2}O_{3-\delta}$ sample has the highest conductivity in both air and CO_2 atmosphere, and the structure is more stable in CO_2 for the other samples. Therefore, the structure of the $BaCe_{0.8}Y_{0.2}O_{3-\delta}$ sample in water was further investigated. It is impossible to restrain the chemical reaction between $BaCe_{0.8}Y_{0.2}O_{3-\delta}$ and water due to the negative Gibb's free energy of this reaction below 403 °C. However, it is possible to decrease the reaction rate. The XRD patterns of $BaCe_{0.8}Y_{0.2}O_{3-\delta}$ exposed to a water vapor-rich environment at 80 °C at different durations are shown in Fig. 8. It was found that the structure of $BaCe_{0.8}Y_{0.2}O_{3-\delta}$ is stable below 2 h. There is only a small amount of $Ba(OH)_2$ phases formed at 4 h, as the time increases to 6 h, the $Ba(OH)_2$ and CeO_2 phases are clearly observed. The perovskite main structure of $BaCe_{0.8}Y_{0.2}O_{3-\delta}$ almost disappeared

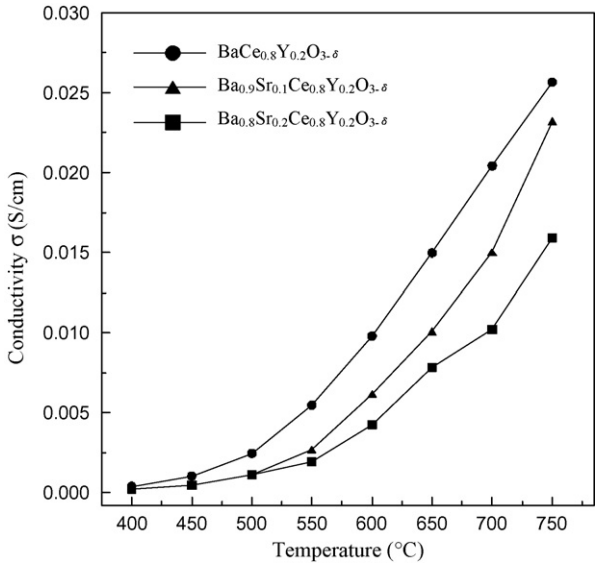

Fig. 9. Conductivity of $Ba_{1-y}Sr_yCe_{0.8}Y_{0.2}O_{3-\delta}$ at different temperatures in air.

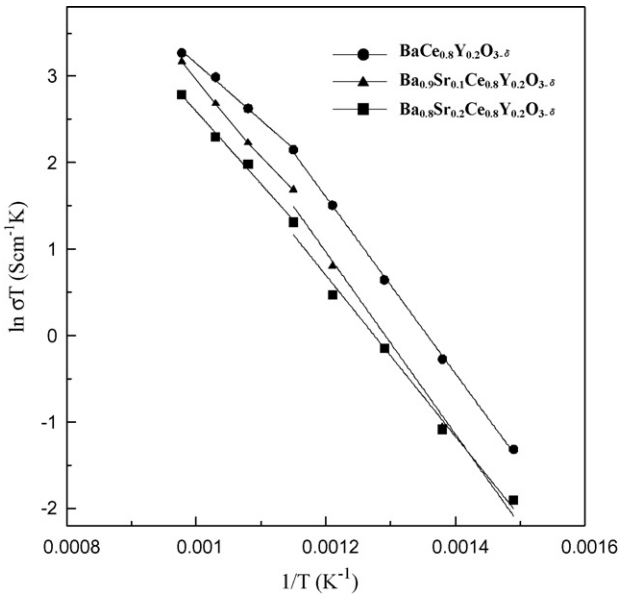

Fig. 10. Arrhenius plot of $Ba_{1-y}Sr_yCe_{0.8}Y_{0.2}O_{3-\delta}$ at different temperature in 3 RH% air humidity atmosphere.

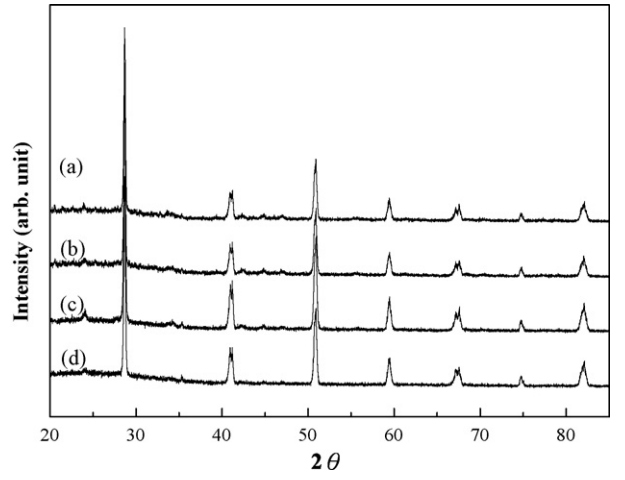

Fig. 11. XRD patterns of $Ba_{0.9}Sr_{0.1}Ce_{0.8}Y_{0.2}O_{3-\delta}$ exposed to a water vapor-rich environment at 80 °C for (a) 8 h, (b) 6 h, (c) 4 h, and (d) 2 h.

completely and reacted into the $Ba(OH)_2$ and CeO_2 phase with water.

In order to improve the structural stability of $BaCe_{0.8}Y_{0.2}O_{3-\delta}$ in water, Sr-doped $BaCe_{0.8}Y_{0.2}O_{3-\delta}$ samples were prepared. Fig. 9 shows the conductivity of $Ba_{1-y}Sr_yCe_{0.8}Y_{0.2}O_{3-\delta}$ (y = 0–0.2) in air. The conductivity of $Ba_{1-y}Sr_yCe_{0.8}Y_{0.2}O_{3-\delta}$ (y = 0–0.2) samples decreased with the doping amount of Sr. The conductivity of $Ba_{0.9}Sr_{0.1}Ce_{0.8}Y_{0.2}O_{3-\delta}$ and $Ba_{0.8}Sr_{0.2}Ce_{0.8}Y_{0.2}O_{3-\delta}$ was 0.023 and 0.016 S cm^{-1} at 750 °C, which is lower by about 12% and 31% than that of $BaCe_{0.8}Y_{0.2}O_{3-\delta}$, respectively. Fig. 10 gives an Arrhenius plot of the conductivity of $Ba_{1-y}Sr_yCe_{0.8}Y_{0.2}O_{3-\delta}$ (y = 0–0.2) samples at 400–750 °C in air. There are still two conductivity mechanisms from proton conductivity change to oxygen conductivity at about 600 °C. The XRD patterns of $Ba_{0.9}Sr_{0.1}Ce_{0.8}Y_{0.2}O_{3-\delta}$ exposed to a water vapor-rich environment at 80 °C at different duration is shown in Fig. 11. It was found that the main perovskite of $Ba_{0.9}Sr_{0.1}Ce_{0.8}Y_{0.2}O_{3-\delta}$ still remains and no $Ba(OH)_2$ and CeO_2 impure phases were formed after 8 h. This result indicates that the structure of $Ba_{0.9}Sr_{0.1}Ce_{0.8}Y_{0.2}O_{3-\delta}$ is much more stable than that of $BaCe_{0.8}Y_{0.2}O_{3-\delta}$ in water. To compare the phase stability of $Ba_{0.9}Sr_{0.1}Ce_{0.8}Y_{0.2}O_{3-\delta}$ prepared in this study with the $Ba_{0.9}Sr_{0.1}Ce_{0.8}Y_{0.2}O_{2.95}$ and $BaCe_{0.7}Zr_{0.2}Y_{0.1}O_{2.95}$ reported by Zhong [15], it was found that the $Ba_{0.9}Sr_{0.1}Ce_{0.8}Y_{0.2}O_{2.95}$ and $BaCe_{0.7}Zr_{0.2}Y_{0.1}O_{2.95}$ decomposed significantly with water 3 h. However, the $Ba_{0.9}Sr_{0.1}Ce_{0.8}Y_{0.2}O_{3-\delta}$ prepared in this study did not decompose with water 8 h. This suggests that the $Ba_{0.9}Sr_{0.1}Ce_{0.8}Y_{0.2}O_{3-\delta}$ is more suitably used as the SOFC electrolyte materials due to its high structural stability; although its conductivity is little lower than that of $BaCe_{0.8}Y_{0.2}O_{3-\delta}$. The electrochemical properties and power performance of a single SOFC cell based on the $Ba_{0.9}Sr_{0.1}Ce_{0.8}Y_{0.2}O_{3-\delta}$ electrolyte are still in process.

4. Conclusions

The $BaCe_{0.8}Y_{0.2}O_{3-\delta}$ exhibits the highest conductivity of 0.026 and 0.025 S cm^{-1} at 750 °C in air and CO_2, respectively. However, the reaction rate of $BaCe_{0.8}Y_{0.2}O_{3-\delta}$ with water is extremely high, and the perovskite structure decomposes into $Ba(OH)_2$ and CeO_2 phases after 8 h in water. $Ba_{0.9}Sr_{0.1}Ce_{0.8}Y_{0.2}O_{3-\delta}$ has slightly lower conductivity, but the structural stability is much better than that of $BaCe_{0.8}Y_{0.2}O_{3-\delta}$. $Ba_{0.9}Sr_{0.1}Ce_{0.8}Y_{0.2}O_{3-\delta}$ exhibits high conductivity of 0.023 S cm^{-1} at 750 °C and the perovskite structure still remains after 8 h in water.

Acknowledgements

The work was supported by the National Science Council of Taiwan (NSC 96-2221-E-155-053 and NSC 97-2221-E-155-059).

References

[1] N.Q. Minh, J. Am. Ceram. Soc. 76 (1993) 563–588.
[2] H. Iwahara, T. Esaka, H. Uchida, N. Maeda, Solid State Ionics 34 (1981) 359–363.
[3] H. Iwahara, H. Uchida, N. Maeda, Solid State Ionics 11 (1983) 109–115.
[4] H. Iwahara, H. Uchida, K. Ono, K. Ogaki, J. Electrochem. Soc. 135 (1988) 529–533.
[5] T. Hibino, A. Hashimoto, M. Suzuki, M. Sano, J. Electrochem. Soc. 149 (2002) A1503–A1508.
[6] B. Zhu, X. Liu, T. Schober, Electrochem. Commun. 6 (2004) 378–383.
[7] S. Yamaguchi, S. Yamamoto, T. Shishido, M. Omori, A. Okubo, J. Power Sources 129 (2004) 4–6;
N. Ito, M. Iijima, K. Kimura, S. Iguchi, J. Power Sources 152 (2005) 200–203.
[8] A. Tomita, S. Teranishi, M. Nagao, T. Hibino, M. Sano, J. Electrochem. Soc. 153 (2006) A956–A960.
[9] Y. Akimune, K. Matsuo, H. Higashiyama, K. Honda, M. Yamanaka, M. Uchiyama, M. Hatano, Solid State Ionics 178 (2007) 575–579.
[10] S. Gopalan, A.V. Virkar, J. Electrochem. Soc. 140 (1993) 1060–1065.
[11] S.V. Bhide, A.V. Virkar, J. Electrochem. Soc. 146 (1999) 2038–2044.
[12] K.H. Ryu, S.M. Haile, Solid State Ionics 125 (1999) 355–367.
[13] S.M. Haile, G. Staneff, K.H. Ryu, J. Mater. Sci. 36 (2001) 1149–1160.
[14] A.K. Azad, J.T.S. Irvine, Solid State Ionics 178 (2007) 635–640.
[15] Z. Zhong, Solid State Ionics 178 (2007) 213–220.
[16] N. Fukatsu, N. Kurita, T. Yajima, K. Koide, T. Ohashi, J. Alloy Compd. 231 (1995) 706–712.
[17] G. Ma, T. Shimura, H. Iwahara, Solid State Ionics 110 (1998) 103–110.
[18] H. Matsumoto, Y. Kawasaki, N. Ito, M. Enoki, T. Ishihara, Electrochem. Solid State Lett. 10 (2007) B77–B80.
[19] H. Iwahara, T. Yajima, H. Ushida, Solid State Ionics 70/71 (1994) 267–271.
[20] A. Tomita, T. Hibino, M. Suzuki, M. Sano, J. Mater. Sci. 39 (2004) 2493–2497.
[21] F.W. Dynys, M.H. Berger, A. Sayir, Solid State Ionics 177 (2006) 2333–2337.